Accepted Manuscript

http://dx.doi.org/10.1002/zaac.201700246

M. Mangstl, V.R. Celinski, C. Pritzel, R. Trettin, and J. Schmedt auf der Günne. Irreversible phase transition of bistetramethylammonium hydrogencyclotriphosphate. *Z. Anorg. Allg. Chem.*, 643:1609--1614, 2017.

Irreversible Phase Transition of Bistetramethylammonium Hydrogencyclotriphosphate

Martin Mangstl,[a] Vinicius R. Celinski,[a] Christian Pritzel,[b] Reinhard Trettin[b] and Jörn Schmedt auf der Günne*[a]

Dedicated to Professor Wolfgang Schnick on the Occasion of his 60th Birthday

Abstract: Crystalline α-bistetramethylammonium hydrogencyclotriphosphate $[N(CH_3)_4]_2HP_3O_9$ (*Pcab*) which had been synthesized via a low-temperature route (<60 °C) shows an irreversible 1st order phase transition to β-$[N(CH_3)_4]_2HP_3O_9$ ($P2_12_12_1$) which was investigated by differential scanning calorimetry, x-ray powder diffraction and solid state nuclear magnetic resonance spectroscopy. The crystal structure of β-bistetramethylammonium hydrogencyclotriphosphate was solved and refined from x-ray powder diffraction data by the Rietveld method using constraints obtained by ^{31}P, ^{1}H and ^{13}C NMR spectroscopy. The new compound crystallizes in an orthorhombic space group with a = 9.3828(1), b = 11.8196(1) and c = 16.0396(2) Å.

Introduction

Inorganic and organic phosphates are widely used in industry and for medical applications, for example as implant coatings and tissue engineering,[1–3] flame retardant additives,[4–6] cathode materials in rechargeable batteries[7–9] and ion conductors.[10–12] A special role play proton ion conductors which are developed for fuel cells, sensor applications and hydrogen separation.[13–16] A highlight is a high-temperature phase of CsH_2PO_4 which is a fast solid-state protonic ionic conductor.[17]

One motivation to synthesize tetramethylammonium phosphates lies in the concept of the tetramethylammonium cation as a super-sized alkali ion. Due to a bigger ionic radius of the tetramethylammonium cation versus the biggest stable alkali ion Cs^+, the Coulomb interaction between anions and cations is weaker and interesting properties can be expected, which may help in finding good ion conductors or glass systems with low-lying glass transition temperatures. A problem of the tetramethylammonium ion is its low thermal stability. Tetramethylammonium salts decompose at temperatures between about 250 to 350 °C depending on the system. Thus a low temperature synthesis route is a special requirement. The synthesis of salts of organic cations of water-free phosphate salts can be achieved by synthesis from the reaction of P_4O_{10} with nitrate salts of the required cation in dimethylsulfoxide DMSO.[18] Corresponding to the sensitivity of the tetramethylammonium cation only few other crystalline phosphates are known, which have been produced by precipitation from aqueous solution, i.e. dihydrogenphosphate hemihydrate $[N(CH_3)_4]H_2PO_4 \cdot 0.5\ H_2O$ and tetramethylammonium dihydrogenphosphate monohydrate $[N(CH_3)_4]H_2PO_4 \cdot H_2O$.[19,20]

In this article we investigate the phase transition from α- to β-bistetramethylammonium hydrogencyclotriphosphate $[N(CH_3)_4]_2HP_3O_9$ by means of differential scanning calorimetry (DSC), X-ray powder diffraction (XRD) and solid state nuclear magnetic resonance (NMR) spectroscopy.

* Prof. Dr. J. Schmedt auf der Günne
E-mail: guenne@chemie.uni-siegen.de
[a] Inorganic Materials Chemistry
University of Siegen
Adolf-Reichwein-Straße 2, 57076 Siegen
[b] Prof. Dr. R. Trettin
Institute for Building and Materials Chemistry
University of Siegen
Paul-Bonatz-Straße 9-11, 57076 Siegen

Experimental Section

General Remarks

All solid educts were stored inside a glove box (MBraun, Garching, Germany) filled with dry argon. Every synthesis step was done under argon atmosphere using air-free techniques. For synthesis of α-bistetramethylammonium hydrogencyclotriphosphate as reported in reference [18] 2.5 mmol (354.8 mg) phosphorus pentoxide (Riedel de Haën, 99 %) and 5.0 mmol (680.8 mg) tetramethylammonium nitrate (Alfa Aesar, 98 %) were mixed. Subsequently, 10 mL dimethyl sulfoxide (Sigma Aldrich, anhydrous, > 99.9 %) was added dropwise under ice cooling. After reaching room temperature the suspension was heated to 58 °C for twelve hours. The obtained product was precipitated and washed five times with acetonitrile (Sigma Aldrich, 99.9 %). A colorless powder was obtained. In order to receive β-bistetramethylammonium hydrogencyclotriphosphate the obtained powder was heated up to 210 °C for 1 h. Again a colorless powder was gained.

NMR Spectroscopy

For all solid-state measurements the ^{1}H resonance of 1 % $Si(CH_3)_4$ in $CDCl_3$ served as an external secondary reference using the Ξ values for ^{13}C and ^{31}P as reported by the IUPAC.[21] All experiments used a saturation pulse comb in front of every repetition delay.

The ^{1}H and ^{31}P solid-state double-resonance NMR spectra were measured on a Bruker Avance III spectrometer operating at the frequencies of 500.25 and 202.51 MHz, respectively (magnetic flux density B_0 = 11.7 T). Magic angle sample spinning (MAS) was carried out with a commercial 2.5 mm double resonance MAS probe. The ^{1}H MAS NMR spectrum was recorded at a sample spinning frequency of 25 kHz with a repetition delay of 8 s. The 2D ^{31}P-^{1}H-heteronuclear-correlation MAS NMR spectrum was recorded at ambient temperature. The spectrum was obtained with a 2D correlation experiment based on the PRESTO-II pulse sequence[22] as described in reference [23]. Here, proton decoupling was implemented using TPPM decoupling with a

nutation frequency of 115 kHz. The nutation frequency for the $R18_5^2$ recoupling sequence used a ^{1}H nutation frequency of 112.5 kHz for the R-elements which consisted of simple π-pulses. All other hard pulses used on both channels were implemented with a nutation frequency of 100 kHz. We used rotor synchronized t_1 increments for all 2D experiments and acquired data according to the States method.[24]

The following ^{13}C and ^{31}P MAS NMR spectra were measured on a Bruker Avance II spectrometer operating at the frequencies 50.34 and 81.03 MHz, respectively (B_0 = 4.7 T). The ^{31}P{^{1}H} MAS NMR spectrum was obtained at a sample spinning frequency of 6 kHz with a repetition delay of 128 s. Proton decoupling was implemented using continuous wave (CW) decoupling with a nutation frequency of 100 kHz. The ^{31}P-^{31}P 2D double-quantum (DQ) single-quantum (SQ) correlation MAS NMR spectrum was obtained at a sample spinning frequency of 6 kHz with a repetition delay of 9 s using a transient adapted PostC7 sequence[25,26] with a conversion period of 1.3 ms and rotor-synchronized data sampling of the indirect dimension. It accumulated 96 transients/FID. Proton decoupling was implemented using CW decoupling with a nutation frequency of 120 kHz. Moreover the ^{13}C{^{1}H} spectrum based on ramped cross-polarization[27] with magic angle spinning was obtained at a sample spinning frequency of 5 kHz with a recycle delay of 12 s. Proton decoupling was achieved using TPPM decoupling with a nutation frequency of 22 kHz.

The ^{31}P{^{1}H} liquid-state NMR spectrum was recorded on a Jeol Eclipse 270 spectrometer operating at the frequencies of 109.27 and 269.94 MHz, respectively (B_0 = 6.34 T). ^{1}H and ^{31}P chemical shifts were referenced to the solvent signal as secondary internal standard.

Powder X-ray diffraction

The powder X-ray diffraction pattern of β-$[N(CH_3)_4]_2HP_3O_9$ was recorded at 298 K on a STOE Stadi P powder diffractometer (STOE, Darmstadt, Germany) in Debye–Scherrer geometry (capillary inner diameter: 0.48 mm) by using Ge(111)-monochromated $CuK_{\alpha1}$ radiation (154.0596 pm) and a position-sensitive detector. Extraction of the peak positions and pattern indexing were carried out by using the TOPAS package.[28] Indexing by using the SVD method yielded an orthorhombic unit cell with the best goodness of fit (GoF) for space group $P2_12_12_1$ with a = 11.8130, b = 9.3783 and c = 16.0327 Å. The ten best solutions are shown in Table 1.

After indexing and LeBail fitting, all the likely space groups are subjected to a "multiple world simulation" within the FOX[29] program. Structure solution was done with the method "parallel tempering". Again the space group $P2_12_12_1$ with a = 11.8130, b = 9.3783 and c = 16.0327 Å shows by far the lowest cost function and is for this reason the best solution (Table 1). The molecules were restrained in different ways: cyclic phosphate units with the flexibility model "automatic from restraints, strict" and tetramethylammonium units with the flexibility model "rigid bodies". The molecules chosen reflect the prior knowledge due to the NMR experiments. Rietveld refinement of the final structure model was realized by applying the fundamental parameter approach implemented in TOPAS (direct convolution of source emission profiles, axial instrument contributions, crystallite size and micro-strain effects).[30]

Table 1. Indexing and structure solution results for β-$[N(CH_3)_4]_2HP_3O_9$.

space group	GoF / indexing	Cost / solution	a / Å	b / Å	c / Å
$P2_12_12_1$	36.46	19939	11.8130	9.3783	16.0327
$P2_12_12$	34.70	61598	11.8130	9.3783	16.0327
$P222_1$	34.15	75168	11.8130	9.3783	16.0327
$P222$	32.59	97877	11.8130	9.3783	16.0327
$P2_12_12_1$	10.98	131988	15.9456	11.7792	9.3361
$P2_12_12_1$	10.85	127647	15.9451	11.7561	9.3364
$P2_12_12_1$	10.52	136660	11.7671	9.3320	15.9415
$P2_12_12_1$	10.01	126443	11.7481	15.9477	9.3385
$P2_12_12_1$	9.85	132170	15.9813	9.3350	11.7452
$P2_12_12_1$	9.77	130065	11.7474	15.9450	9.3366

It is difficult to determine the hydrogen positions by powder X-ray diffraction because of the low scattering power of hydrogen atoms. Therefore the hydrogen positions were constrained based on neutron diffraction analysis data of a known tetramethylammonium salt. For the tetramethylammonium cation the bond lengths of C-H were constrained to 0.96 Å (as proposed by Sheldrick) and N-C-H angles to 108.4 ° (average value of a tetramethylammonium salt via neutron diffraction analysis given in reference [31]). The position of H52 was constrained to the center of the straight line between O2 and O5' from a neighboring cyclotriphosphate unit. This is consistent with the presence of a strong (linear) hydrogen bond.[32] For terminal P-O distances soft restraints were used on the basis of an average value of a known cyclotriphosphate.[33] The crystallographic data and further details of the data collection are given in Table 2. The experimental powder diffraction pattern, the difference profile of Rietveld refinement and peak positions are shown in Figure 1.

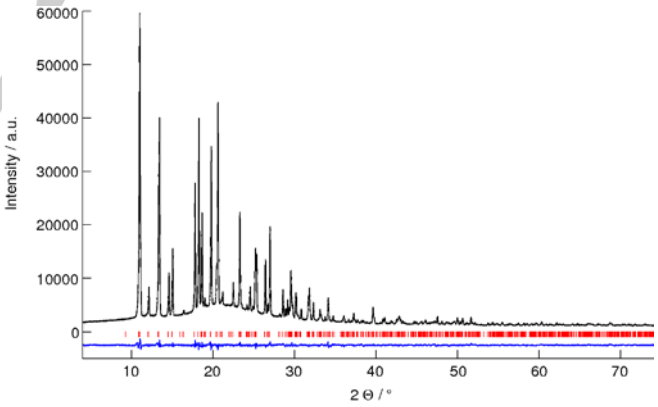

Figure 1. Observed (black line) powder diffraction pattern of β-$[N(CH_3)_4]_2HP_3O_9$ measured with $CuK_{\alpha1}$ radiation (154.0596 pm), as well as the difference profile (blue line) of the Rietveld refinement. Peak positions are marked by vertical red lines.

Table 2. Crystallographic data[a] for β-$[N(CH_3)_4]_2HP_3O_9$.

crystal structure data

formula	$H_{25}C_8P_3O_9N_2$
formula mass /(g mol^{-1})	386.213
crystal system	orthorhombic
space group	$P2_12_12_1$ (no. 19)
a / Å	9.3828(1)
b / Å	11.8196(1)
c / Å	16.0396(2)
cell volume / Å^3	1778.80(3)
Z	4
ρ / (g/cm^3) calq. from XRD	1.44216(2)
data collection	
diffractometer	Stoe Stadi P
radiation, monochromator	CuK$_{\alpha1}$, λ=154.06pm, Ge(111)
detector, internal step width / °	Linear PSD (Δ(2θ)=5°), 0.01
temperature / K	294(2)
2θ range / °	4.0 - 73.99
step width / °	0.01
points	7000
number of observed reflections	555
structure refinement	
structure refinement method	fundamental parameter model[30]
program used	TOPAS-Academic 4.1
background function/parameters shifted	Chebyshev / 24
number of atomic parameters	90
number of profile and other parameters	7
constraints/restraints	68/26
χ2	1.611
R_p	0.0692
wR_p	0.0291
R_p	0.0692

[a] Estimated standard deviations are given in parentheses.

Differential scanning calorimetry

Differential scanning calorimetry measurements were done on a Netzsch DSC 204 F1 calorimeter (Netsch, Selb, Germany). An amount of 7.00 mg of the sample was sealed within an aluminum crucible inside a glove box under argon atmosphere. The measurements were carried out under nitrogen atmosphere (20 mL/min) with a heating- and cooling rate of 5 K/min.

Results and Discussion

The structure of β-$[N(CH_3)_4]_2HP_3O_9$ was characterized by X-ray diffraction and NMR spectroscopy. Several unsuccessful attempts were made to grow single crystals of sufficient size for single-crystal X-ray diffraction experiments. Therefore the structure solution had to start from X-ray powder diffraction data. The strategy we followed to obtain the crystal structure was to first obtain diverse constraints by solid-state and liquid-state NMR about the crystalline product of the phase transformation and then use these constraints for a structure solution and refinement by XRD.

The $^{31}P\{^1H\}$ liquid NMR spectrum of β-$[N(CH_3)_4]_2HP_3O_9$ dissolved in D_2O features a main signal with a chemical shift of −20.94 ppm. This is in agreement with the chemical shift of a cyclotriphosphate.[34] The easy dissolution of the sample in water and the ^{31}P NMR peaks of the solution can only be explained by the presence of molecular ions rather than by chainlike phosphates.

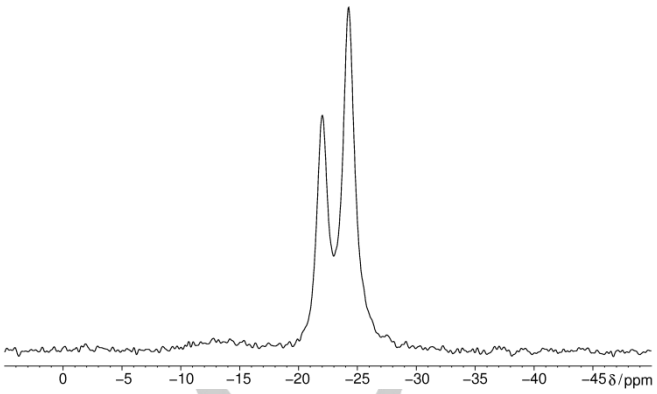

Figure 2. Isotropic signals in a quantitative ^{31}P MAS NMR spectrum of β-$[N(CH_3)_4]_2HP_3O_9$ obtained at a sample spinning frequency of 6 kHz. The spectrum shows three signals corresponding to three different crystallographic orbits of phosphorus atoms. One signal appears at −22.0 ppm and two signals at −24.2 ppm are overlapping. A small amount of an amorphous side-phase at −12.7 ppm is observed.

The $^{31}P\{^1H\}$ MAS NMR spectrum of β-$[N(CH_3)_4]_2HP_3O_9$ displays signals of three different crystallographic orbits of phosphorus atoms at −22.0 and −24.2 ppm (Figure 2). Two signals at −24.2 ppm are overlapping. A small amount of an amorphous side-phase at −12.7 ppm is also observed, which typically shows a peak about 4 times as broad as the crystalline peaks. Finally, no signal is visible at δ = −45.9 ppm which indicates that P_4O_{10} reacts quantitatively.

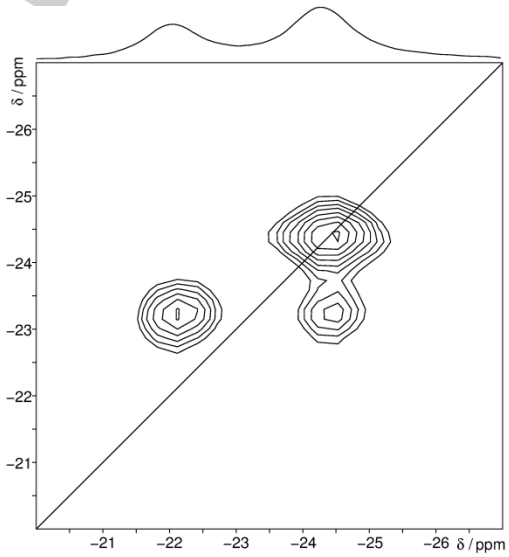

Figure 3. Homonuclear ^{31}P-^{31}P MAS NMR single-quantum double-quantum correlation spectrum of β-$[N(CH_3)_4]_2HP_3O_9$ obtained at a sample spinning frequency of 6 kHz. The 1D projection at the top of the 2D spectrum stems from a separate one-pulse experiment. Correlation peaks are shown via contour plots. The diagonal line refers to the hypothetic peak position of two isochronous spins (autocorrelation diagonal).[25,26]

The homonuclear ^{31}P MAS single-quantum (SQ) double-quantum (DQ) correlation spectrum (Figure 3) indicates that these three signals must belong to the same crystalline phase, due to their correlation peaks. Both this correlation pattern as well as the peak areas are

consistent with that of a cyclotriphosphate and not with that of a cyclotetraphosphate.

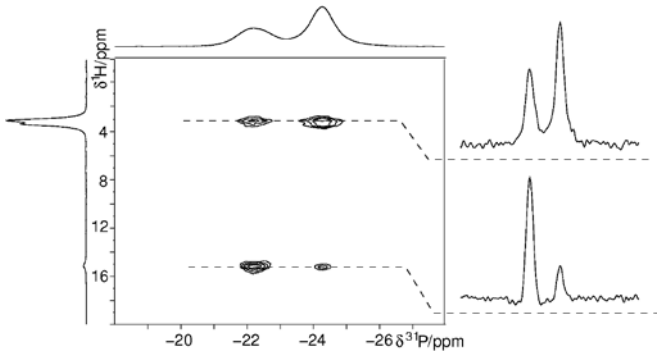

Figure 4. $^{31}P\{^{1}H\}$ Heteronuclear correlation MAS NMR spectrum of β-$[N(CH_3)_4]_2HP_3O_9$ measured at a sample spinning frequency of 25 kHz. Correlation peaks are shown via contour plots.[22,23]

The heteronuclear 2D $^{31}P\{^{1}H\}$ MAS correlation spectrum of β-$[N(CH_3)_4]_2HP_3O_9$ indicates spatial proximity between phosphorus and hydrogen atoms (Figure 4). Only in the case of close ^{31}P-^{1}H vicinity a correlation peak can be observed. Due to the correlation peaks between the ^{1}H signal at 3.4 ppm and all three ^{31}P signals we conclude that every phosphorus site of the cyclotriphosphate is close to a tetramethylammonium molecule. The ^{1}H signal at 15.2 ppm correlates stronger with the ^{31}P peaks at −22.0 ppm and weaker with the ^{31}P peaks at −24.2 ppm. This suggests that the phosphorus site, showing a signal at −22.0 ppm is closer to the hydrogen atom within the strong hydrogen bond than the other two phosphorus sites.

Table 3. ^{1}H, ^{13}C and ^{31}P isotropic chemical shifts δ_{iso}, ^{1}H and ^{31}P normalized peak areas A, ^{1}H and ^{31}P spin–lattice relaxation times T_1 and ^{31}P anisotropic chemical shifts δ_{aniso} for β-$[N(CH_3)_4]_2HP_3O_9$.

	Peak 1	Peak 2	Peak 3
$\delta_{iso}(^{31}P)$ / ppm	−12.7	−22.0	−24.2
δ_{aniso} / ppm	−61	−141	−147
η	0.48	0.28	0.42
$\delta_{11}(^{31}P)$ / ppm	32.4	68.3	80.0
$\delta_{22}(^{31}P)$ / ppm	3.2	28.8	18.4
$\delta_{33}(^{31}P)$ / ppm	−73.7	−163.1	−171.0
$A(^{31}P)$ / a.u.	0.1	1	2.4
$T_1(^{31}P)$ / s	-	4.7	4.2
$\delta_{iso}(^{13}C)$ / ppm	53.8	-	-
$\delta_{iso}(^{1}H)$ / ppm	15.2	3.5	3.3
$A(^{1}H)$ / a.u.	1	8.3	15.6
$T_1(^{1}H)$ / s	-	0.1	0.1

The quantitative ^{1}H MAS NMR spectrum (Figure 5) features two peaks at 3.3 and 3.5 ppm that can be assigned to the tetramethylammonium cation and a peak at 15.2 ppm that is typical for an acidic hydrogen atom within a strong hydrogen bond between oxygen atoms of cyclotriphosphate units. In contrast for α-$[N(CH_3)_4]_2HP_3O_9$ only one signal for tetramethylammonium hydrogen atoms could be observed. The signal intensity ratio of 1 : 23.9 is within error limits consistent with the chemical formula $[N(CH_3)_4]_2HP_3O_9$.

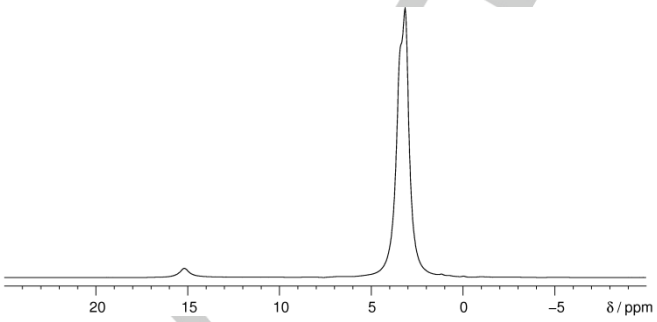

Figure 5. ^{1}H MAS NMR spectrum of β-$[N(CH_3)_4]_2HP_3O_9$ measured at a sample spinning frequency of 25 kHz. The peaks at 3.3 and 3.5 ppm can be assigned to the tetramethylammonium cation and the peak at 15.2 ppm is typical for a hydrogen atom within a strong hydrogen bond.

Structure solution starting from X-ray powder data was helped by the known molecular composition which could be determined via NMR spectroscopy. The composition combined with the unit cell parameters allowed to predict the number of formula units *Z* per unit-cell for each potential model. This turns the structure solution into a simple task. P-atoms on special positions are not to be expected since three crystallographic P-atoms in a single cyclotriphosphate anion became evident through homonuclear ^{31}P 2D and heteronuclear $^{31}P\{^{1}H\}$ 2D NMR spectroscopy (Figure 3 and 4). The technical process of how to obtain the crystal structure is described in the experimental part. All observed reflections were indexed with one crystalline phase on the basis of orthorhombic unit cell parameters a = 11.8130, b = 9.3783 and c = 16.0327 Å. A Rietveld refinement was then performed in space group $P2_12_12_1$ with a structure model that contained three phosphorus, nine oxygen, two nitrogen and eight carbon atoms in the asymmetric unit. This solution is in agreement with both the results from XRD and NMR.

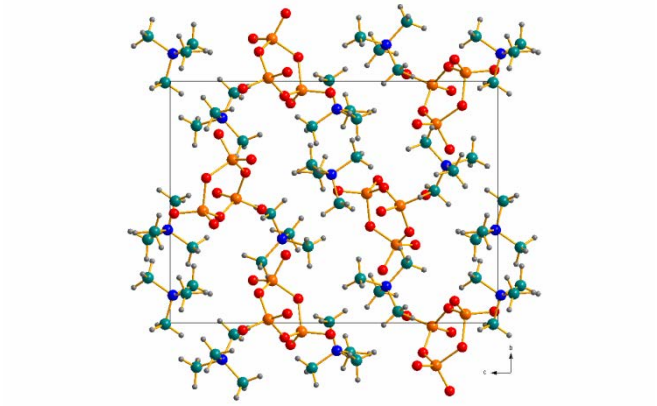

Figure 6. Crystal structure of β-$[N(CH_3)_4]_2HP_3O_9$ viewed along [100]. Orange spheres: phosphorus, red spheres: oxygen, blue spheres: nitrogen, teal spheres: carbon, gray spheres: hydrogen.

The lengths of the bridging P-O-P bonds are between 1.52(1) and 1.67(1) Å, while the terminal P-O bonds vary between 1.41(1) and 1.44(1) Å which is in good agreement with literature data.[33,35,36] Internal P-O-P and O-P-O angles vary between 108.3 and 133.2 ° which also represent reasonable values.[33] The acidic proton is localized in a strong H-bond which can be identified with the shortest intermolecular O-O distance of 2.55 Å. For strong H-bonds a strong correlation between the ^{1}H NMR chemical shift and the O-O distances is known.[37] Within error limits the predicted chemical shift value of approximately 13(±3) ppm agrees well with the observed ^{1}H chemical shift value of 15.2 ppm.

Since the distances between the oxygen atoms of neighboring phosphate units increase only slightly as compared to the metastable α-structure, it is unlikely that this is the driving force to undergo a phase transition.

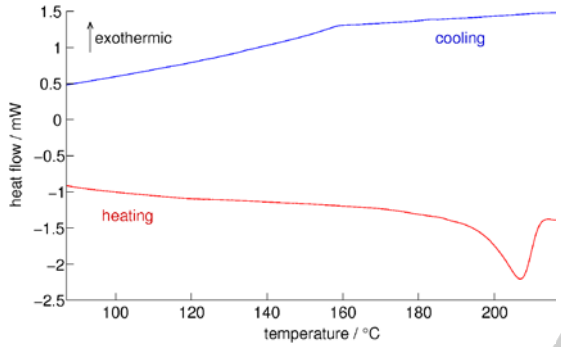

Figure 7. DSC measurement of α-$[N(CH_3)_4]_2HP_3O_9$ between 80 and 220 °C with a heating/cooling rate of 5 K/min (heating: red line, cooling: blue line). Onset temperature of an irreversible phase transition to β-$[N(CH_3)_4]_2HP_3O_9$ during heating at 195.3 °C.

Differential scanning calorimetry shows an irreversible endothermic 1st order phase transition with an onset temperature of 195.3 °C (Figure 7). It can be excluded that the small signal upon cooling with an onset temperature at 158.1 °C belongs to the same phase transition because this signal is also present when the sample is heated only up to 180 °C. It could be explained by the freezing of a motional degree of freedom of rotations of the tetramethylammonium ion. Ultimately, the diffraction pattern of α-bistetramethylammonium hydrogencyclotriphosphate could not be observed after heating above 210 °C which supports the idea of irreversibility of the phase transition. By integration of the signal with a background corrected heating curve the following reaction enthalpy could be determined:

$$\alpha\text{-}[N(CH_3)_4]_2HP_3O_9 \rightarrow \beta\text{-}[N(CH_3)_4]_2HP_3O_9 \qquad \Delta_{trs}H = +5.6\ \text{kJ/mol}$$

Due to a positive value of the enthalpy $\Delta_{trs}H$ the entropy of the system has to increase during the phase transition in order to represent an exergonic reaction. Rotational degrees of freedom of the tetramethylammonium ion could be responsible for this entropic contribution.

Conclusions

The crystal structure of bistetramethylammonium hydrogencyclotriphosphate undergoes an irreversible endothermic 1st order phase transition from a structure describable in space group *Pcab* (α-phase) to a structure describable in space group $P2_12_12_1$ (β-phase) at 195.3 °C. Our structure solution results give no evidence for a static C/N/P/O disorder. The presence of two resolved resonances of the neighboring P-atoms in the NMR spectra indicates that H-ion motion is negligible on the time-scale of the NMR experiment at room temperature. The phase transition illustrates that the chosen low-temperature synthesis route indeed is able to give access to metastable phosphates, which may help to give access to new water-free porous phosphates and phosphates with temperature sensitive cations.

Acknowledgements

We thank Peter Mayer (University of Munich) for technical support with liquid state NMR measurements. We thank Dr. Johannes Weber for helping with computer-related problems.

Keywords: Rietveld refinement • phase transition • NMR • crystal structure • hydrogen bond

References

[1] S. Pina, J. M. Oliveira, R. L. Reis, *Adv. Mater.* **2015**, *27*, 1143–1169.
[2] R. Z. LeGeros, J. P. LeGeros, *Key Eng. Mater.* **2003**, *240–242*, 3–10.
[3] S. V. Dorozhkin, M. Epple, *Angew. Chem. Int. Ed Engl.* **2002**, *41*, 3130–3146.
[4] I. van der Veen, J. de Boer, *Chemosphere* **2012**, *88*, 1119–1153.
[5] S. V. Levchik, E. D. Weil, *J. Fire Sci.* **2006**, *24*, 345–364.
[6] Y. E. Hyung, D. R. Vissers, K. Amine, *J. Power Sources* **2003**, *119–121*, 383–387.
[7] L.-X. Yuan, Z.-H. Wang, W.-X. Zhang, X.-L. Hu, J.-T. Chen, Y.-H. Huang, J. B. Goodenough, *Energy Environ. Sci.* **2011**, *4*, 269–284.
[8] A. K. Padhi, K. S. Nanjundaswamy, J. B. Goodenough, *J. Electrochem. Soc.* **1997**, *144*, 1188–1194.
[9] W.-J. Zhang, *J. Power Sources* **2011**, *196*, 2962–2970.
[10] P. Knauth, *Solid State Ion.* **2009**, *180*, 911–916.
[11] J. Fu, *J. Mater. Sci.* **1998**, *33*, 1549–1553.
[12] M. Cretin, P. Fabry, *J. Eur. Ceram. Soc.* **1999**, *19*, 2931–2940.
[13] G. Alberti, M. Casciola, *Solid State Ion.* **2001**, *145*, 3–16.
[14] K. D. Kreuer, *Annu. Rev. Mater. Res.* **2003**, *33*, 333–359.
[15] T. Norby, *Solid State Ion.* **1999**, *125*, 1–11.
[16] J. W. Phair, S. P. S. Badwal, *Ionics* **2006**, *12*, 103–115.
[17] G. Kim, J. M. Griffin, F. Blanc, S. M. Haile, C. P. Grey, *J. Am. Chem. Soc.* **2015**, *137*, 3867–3876.
[18] M. Mangstl, V. R. Celinski, S. Johansson, J. Weber, F. An, J. Schmedt auf der Günne, *Dalton Trans.* **2014**, *43*, 10033–10039.
[19] K. Fujita, D. R. MacFarlane, K. Noguchi, H. Ohno, *Acta Crystallogr. Sect. E Struct. Rep. Online* **2009**, *65*, o797–o797.
[20] N. Ohama, M. Machida, T. Nakamura, Y. Kunifuji, *Acta Crystallogr. C* **1987**, *43*, 962–964.
[21] R. K. Harris, E. D. Becker, S. M. Cabral de Menezes, P. Granger, R. E. Hoffman, K. W. Zilm, *Pure Appl. Chem.* **2008**, *80*, 59–84.
[22] X. Zhao, W. Hoffbauer, J. Schmedt auf der Günne, M. H. Levitt, *Solid State Nucl. Magn. Reson.* **2004**, *26*, 57–64.
[23] Y. S. Avadhut, J. Weber, E. Hammarberg, C. Feldmann, J. Schmedt auf der Günne, *Phys. Chem. Chem. Phys.* **2012**, *14*, 11610–11625.
[24] D. J. States, R. A. Haberkorn, D. J. Ruben, *J. Magn. Reson.* **1982**, *48*, 286–292.
[25] M. Hohwy, H. J. Jakobsen, M. Edén, M. H. Levitt, N. C. Nielsen, *J. Chem. Phys.* **1998**, *108*, 2686–2694.
[26] J. Weber, M. Seemann, J. Schmedt auf der Günne, *Solid State Nucl. Magn. Reson.* **2012**, *43–44*, 42–50.
[27] G. Metz, X. L. Wu, S. O. Smith, *J. Magn. Reson. A* **1994**, *110*, 219–227.
[28] A. A. Coelho, *TOPAS-Academic*, Coelho Software, Brisbane, Australia, **2007**.
[29] V. Favre-Nicolin, R. Černý, *J. Appl. Crystallogr.* **2002**, *35*, 734–743.
[30] J. Bergmann, R. Kleeberg, A. Haase, B. Breidenstein, *Mater. Sci Forum* **2000**, *347–349*, 303–308.
[31] F. A. Cotton, P. C. W. Leung, W. J. Roth, A. J. Schultz, J. M. Williams, *J. Am. Chem. Soc.* **1984**, *106*, 117–120.
[32] T. Steiner, *Angew. Chem.* **2002**, *114*, 50–80.
[33] M. Jansen, D. Hanke, *Z. Kristallog. – Cryst. Mater.* **1995**, *210*, 610.
[34] T. Glonek, J. R. Van Wazer, M. Mudgett, T. C. Myers, *Inorg. Chem.* **1972**, *11*, 567–570.

[35] M. T. Averbuch-Pouchot, J. C. Guitel, A. Durif, *Acta Crystallogr. C* **1983**, *39*, 809–810.
[36] M. Weil, R. Glaum, *Acta Crystallogr. C* **1997**, *53*, 1000–1003.
[37] J. P. Yesinowski, H. Eckert, *J. Am. Chem. Soc.* **1987**, *109*, 6274–6282.

Entry for the Table of Contents (Please choose one layout)

Layout 1:

FULL PAPER

Text for Table of Contents

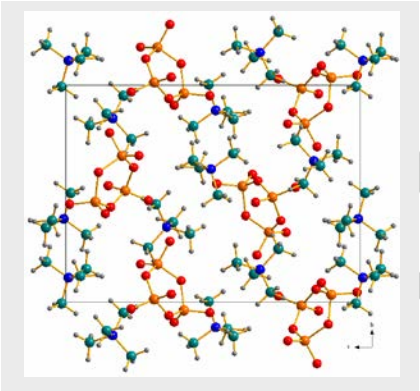

*Martin Mangstl, Vinicius R. Celinski, Christian Pritzel, Reinhard Trettin and Jörn Schmedt auf der Günne**

Page No. – Page No.

Irreversible Phase Transition of Bistetramethylammonium Hydrogencyclotriphosphate

Additional Author information for the electronic version of the article.

Author: ORCID identifier
Author: ORCID identifier
Author: ORCID identifier